Polar
Geophysical
Institute

RELATIVISTIC ELECTRON PRECIPITATION AS SEEN BY NOAA POES

A.G. Yahnin, T.A. Yahnina, N.V. Semenova, B.B. Gvozdevsky *(Polar Geophysical Institute, Apatity)*

Abstract. We performed a survey of relativistic electron precipitation (REP) events, which had been seen with MEPED P6 telescope onboard NOAA POES during a 38-days interval. Combining P6 data with simultaneous energetic (>30 keV) electron and proton observations we divided all REP events into three groups. One group consists of REP enhancements forming the isotropy zone at the poleward edge of relativistic electron fluxes. These REP events are observed on the night side, and are, evidently, produced by isotropization process related to non-adiabatic motion of particles in the stretched night side magnetic field. Second group consists of REP events related to simultaneous enhancements of energetic >30-300 keV electrons. These events have a wider MLT range of occurrence with maximum in the pre-midnight sector. These REP events can be related to interaction of electrons with waves in a wide range of frequencies. Some REP events correlate with burst-like precipitation of >30-keV protons. Such proton bursts indicate the location of the EMIC wave source. Thus, these REP events could be related to scattering of the relativistic electrons by EMIC waves. However, even in such cases the relativistic electrons are always associated with precipitations of energetic (>30 keV) electrons. This fact poses a question: If the relativistic electrons are indeed precipitated by EMIC waves or some other waves precipitating electrons in a wide range of energies are involved?

1. Introduction

Investigation of the relativistic electron precipitation (REP) morphology is important because of the REP atmospheric impact and because it may help in solving the problem of mechanisms of radiation belt losses.

Imhof et al. (1991) using the data from three-axis-stabilized S81-1 spacecraft concluded that REP at the outer limit of electron trapping is due to the particle scattering in that region of the magnetosphere where the radius of the field line curvature is comparable with the gyroradius of the electron (e.g. *Sergeev and Tsyganenko, 1982*).

Another study by *Imhof at al.* (1986) based on the data from several low-orbiting satellites dealt with narrow (with duration of equal or less than 10 s) spikes of relativistic electrons well inside the trapping boundary. Some of these electron spikes were associated with energetic (tens of keV) protons flux enhancements. The authors concluded that the precipitation was due to cyclotron interaction of radiation belt particles with low-frequency waves. Some of the REP spikes were observed near noon, and most of the events including those associated with energetic proton precipitation were found in the late evening sector.

Nakamura et al. (2000) presented the morphology of the precipitation of > 1 MeV electrons based on *SAMPEX* observations. These authors divided REP events into three categories relatively to their duration (<1 s, <10 s, and <30 s). The first category (microbursts) was observed mainly in the morning sector during magnetic storms. MLT distributions of REP bursts with the duration <10 s and <30 s were found to be similar. Their occurrence maximum was in pre-midnight hours for non-storm time, and they were observed at all MLTs during storms.

NOAA Polar-orbiting Operational Environmental Satellites (POES) data have been already used in some statistical studies of REP. Thus, global distribution and variations of the intensity of the ~1 MeV electron precipitation during geomagnetic storms were presented by *Horne et al.* (2009). They found the enhanced precipitation in the vicinity of the South Atlantic Magnetic Anomaly (SAMA) and nearly uniform distribution of the precipitating flux intensity around the pole. Recently, *Carson et al.* (2012) and Wang et al. (2014) constructed maps of occurrence of those REP events, which associate with the localized precipitation of energetic (30-80 keV) protons. The localized precipitation of energetic protons equatorward of the isotropy boundary is suggested to be a signature of the interaction of the ring current/plasma sheet protons with EMIC waves (e.g., *Yahnin and Yahnina, 2007*). Due to huge amount of data (12 years of observations of several satellites), *Carson et al.* applied an automated algorithm for the event selection. Surprisingly, the revealed map of occurrence of "EMIC driven" REP events showed a maximal occurrence on the night side. This seems to be inconsistent with both theoretical predictions and observational statistics of the location of EMIC waves, which could be responsible for scattering of the relativistic electrons (*Thorne and Kennel, 1971; Jordanova et al., 2008; Chen et al., 2009, Meredith et al., 2003*). *Wang et al.* (2014) revisited the Carson's et al. study using more rigorous algorithm of the event selection and revealed the maximal occurrence of the "EMIC driven" REP events in the evening sector.

In this paper advantages of the multi-spacecraft MLT coverage by NOAA POES will be used to study the REP morphology and to compare it with results of some previous studies. To distinguish between REP events of different nature we will use not only data from detectors measuring relativistic electrons (P6), but also measurements of energetic (>30 keV) protons and electrons.

Bellow (section 2) we present the used data and selection criteria. In section 3 three kinds of REP observed with NOAA POES as well as their morphological features are described. A discussion is presented in section 4.

2. Data

The data base used in this study consists of observations of four NOAA satellites (*NOAA-15, -16, -17,* and *–18*) frying at altitude ~800 km during the interval from 25 July to 31 August 2005, which is characterized by the variable geomagnetic activity.

To measure charged particles with energy E>30 keV, NOAA POES are equipped with the Medium Energy Proton and Electron Detector (MEPED) instrument (*Evans and Greer, 2004*). This instrument consists, particularly, of two pairs of directional telescopes. The directional telescopes are oriented such that they sample from the local vertical (zenith) and horizontal ("backwards" along the direction of travel) fields of view (0-degree and 90-degree telescopes, respectively). At sufficiently high latitudes 0-degree telescopes measure precipitating (within the loss cone) particles, while 90-degree telescopes measure particles, which are just outside the loss cone at the equatorial plane (e.g. *Rodger et al., 2010*). Electron telescopes have three nominal energy channels: E1 (>30 keV), E2 (>100 keV), and E3 (>300 keV). Proton directional telescopes are designed to measure ions in six channels: P1 (30-80 keV), P2 (80-250 keV), P3 (250-800 keV), P4 (800-2500 keV), P5 (2500-6900 keV), and P6 (>6.9 MeV). Measurements of protons in the channel P6 are rare, but it is contaminated with relativistic (>700 keV) electrons (e.g., *Yando et al., 2011*). Situation with the relativistic electron contamination can be easily distinguished from the proton event by comparison with counts in the channel P5, which is not contaminated by electrons. If there are no particles detected in P5, the particles observed in P6 are relativistic electrons.

This criterion (the lack of response in P5 during a detectable signal in the 0-degree telescope of the channel P6) was used to select REP events. Following to *Carson et al.* (2012), we excluded from the consideration those NOAA POES passes, which were in the vicinity of SAMA. The sampling rate of the 0- and 90 degree detectors of the MEPED instrument is 2 s (each detector alternately accumulates the signal during one second). Thus, it is clear that NOAA POES are not appropriate for investigation of microbursts. We considered an enhancement of the relativistic electron precipitating flux as the event if its duration was at least 4 seconds (two samples). In all, 209 REP events were selected during the interval under study having the duration from 4 to 32 seconds.

Fig. 1 presents some examples of the 0- and 90-degree fluxes of particles registered in some channels of the MEPED instrument. The upper panel shows the data from channel P1 (Ep=30-80 keV), second and third panels show the fluxes of electrons in channels E1 (Ee>30 keV) and E3 (Ee>300 keV), respectively. The data from channel P6 (Ee>700 keV) are shown at the bottom.
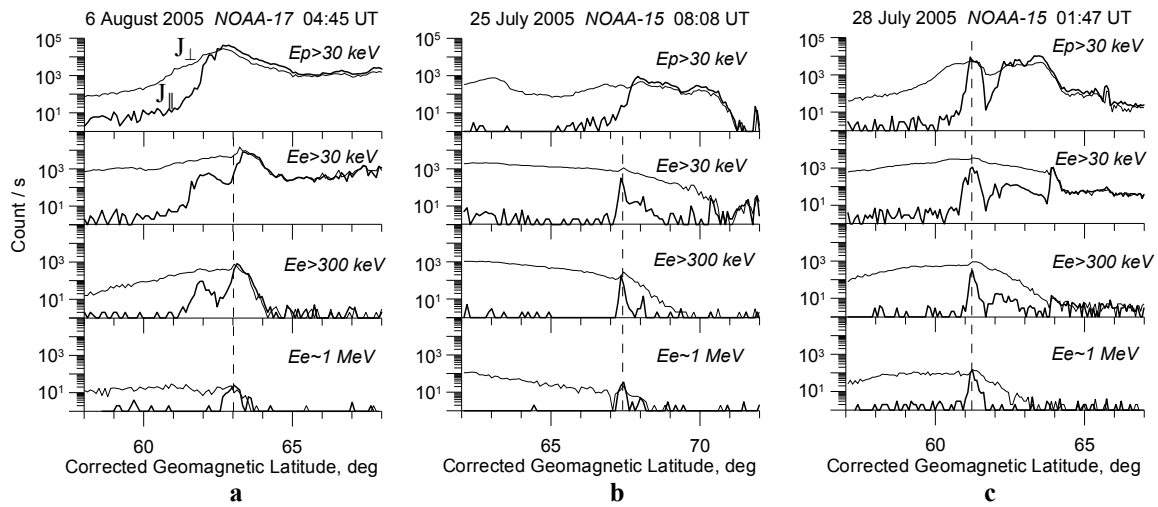
Figure 1

3. Results

Careful inspection of selected REP events enables us to divide them into three groups. The first group is represented by events of isotropization of fluxes (that is, equality of the precipitating and 90-degree flux) in the channel P6, which occurs right at the poleward (outer) boundary of the 90-degree flux, and which do not coincide with any enhancement of the 0-degree flux in any other electron channel. An example of the REP event belonged to this group is shown in Fig. 1a. In such cases the fluxes of >30 and >300 keV electrons also demonstrate the isotropization at the trapped boundary, but the latitude of the isotropy boundary (that is, boundary between isotropic and anisotropic fluxes) of electrons measured in channels E1-E3 and P6 exhibits clear energy dispersion. The higher the energy of electrons, the lower the latitude of the isotropy boundary. This suggests that the electron isotropization and precipitation is related to violation of the adiabatic movement, which occurs when the Larmor radius of the particle is comparable with the curvature radius of the magnetic field line in the vicinity of the equatorial plane of the magnetosphere (e.g., *Sergeev and Tsyganenko, 1982*). Note, that the isotropy boundary for 30-80 keV protons is

47

always situated equatorward of that for electrons because the gyroradius of the 30-keV proton is larger than that of the ~1 Mev electron. During the time interval under study, 65 such events (or 31% of all REP events) are found.

The second group consists of REP spikes, which coincide with the enhanced precipitation of >30 keV electrons and do not coincide with any proton precipitation enhancement (Fig. 1b). These REP are observed well within the anisotropic zone of relativistic electrons and on both sides of the isotropy boundary of 30-80 keV protons. This group consists of 117 events (56%).

Finally, there is a group of REP events, which coincide with localized spikes of precipitation of 30-80 keV protons (Fig. 1c). These events occur within the anisotropic zone of relativistic electrons and always equatorward of the isotropy boundary of 30-80 keV protons. Only 27 such events (13% of all REP events) were observed.

In Fig. 2 a map of REP events is shown in the MLT-CGLat coordinates. The majority of REP events is observed at 60°-70° CGLat. The events of the first group are observed around midnight (20-03 MLT) (Fig. 2a). The events of the second group are seen in all MLT, but mainly in the evening and midnight sector (Fig. 2b). The events correlated with the proton precipitation spikes are observed within the 14-23 MLT interval (Fig. 2c).

The occurrence of the REP events mapped onto the equatorial plane is shown in Fig. 3. The occurrence is determined as the ratio of a number of satellite crossings with REP observations to a number of all crossings through a given region (a cell with dimensions equal to 1 R_E of the distance from the Earth and 1 hour of MLT). The maximal occurrence of the REP events of the first and second groups is some 5 % (Fig. 3a,b), and the events of the third group have maximal occurrence as low as ~1% (Fig. 3c).
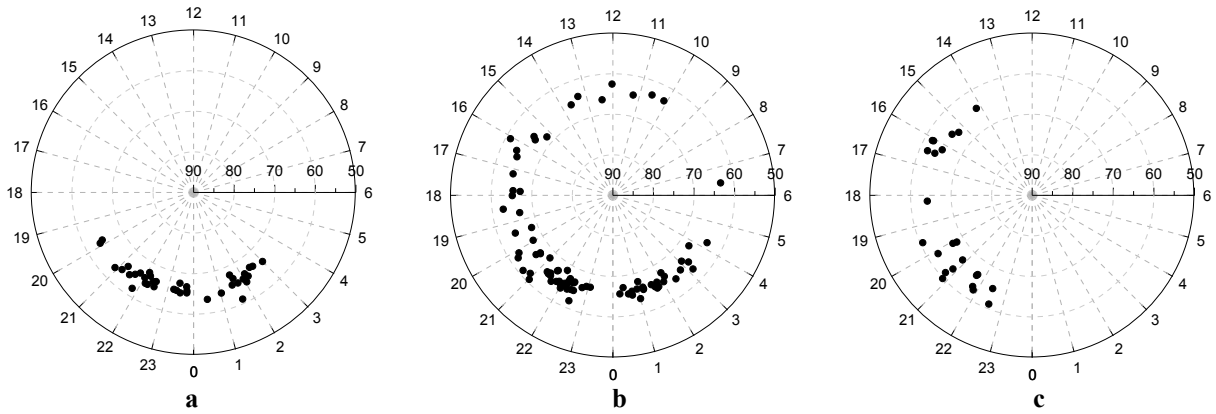
Figure 2
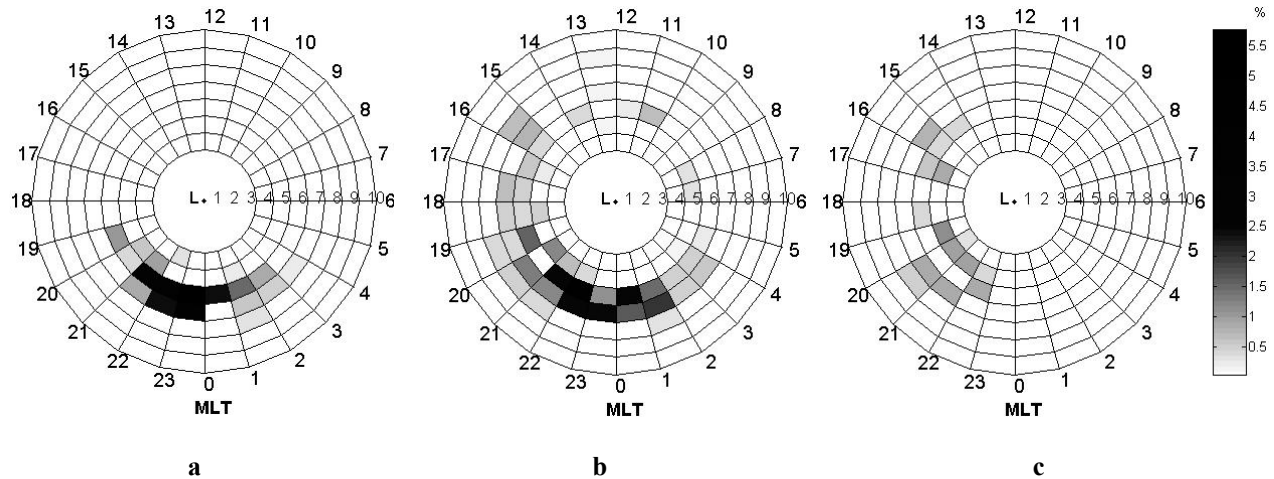
Figure 3

4. Discussion

In some extent, three types of relativistic electron precipitation described above have been studied in earlier works (see, Introduction). Similar study has been made by *Imhof et al.* (1986, 1991) who also used data from polar-orbiting low-altitude satellites. *Imhof et al* (1991) studied REP events at the trapping boundary, which we classified as

belonged to the first group. As already mentioned, these REP events are related to scattering the particles into the loss cone due to violation of the adiabatic motion of particles in the stretched magnetic field in the night side magnetosphere (e.g., *Sergeev and Tsyganenko, 1982*).

Events, which we refer as belonged to group 2 and 3, are similar to spikes of the precipitation studied by *Imhof et al.* (1986). In particular, our Fig. 2 showing the MLT/Latitude distribution of the REP events is similar to their Fig. 9. The distribution of *Imhof et al.* has, however, significant gaps, which are due to the worse, in comparison to our study, coverage of MLTs. It is worth to note that duration of REP events studied by *Imhof et al.* (1986) (<10 s) is less than that in our study (4-32 s). *Nakamura et al.* (2000) compared the morphology of precipitation bursts with a timescale <10 s and <30 s on the basis of SAMPEX data and demonstrated that distributions in L-shell and MLT of these two subsets of events is similar. Most of events are seen between L=4 and 6, and they more often occur in the premidnight sector like it is shown in the present study. Thus, one may conclude that independently on the duration the REP events studied here and those studied by *Imhof et al.* and *Nakamura et al.* have the same nature.

Since REP events of our groups 2 and 3 are well within the trapped population, they cannot be associated with scattering in the stretched magnetic field, but can relate to some wave-particle interaction mechanism. Scattering of the relativistic electrons can be provoked by interaction with whistler mode chorus, hiss emissions, equatorial magnetosonic waves, electromagnetic ion-cyclotron (EMIC) waves (see, *Milan and Thorne, 2007; Thorne, 2010, and references therein*). *Sklyar and Kliem* (2006) argued that electrostatic waves near the upper hybrid resonance (UHR) frequency are capable to effectively precipitate ~1 MeV electrons.

Occurrence of whistler mode chorus is maximal at large distances (L>5) in the dawn-noon sector (e.g. *Meredith et al., 2013*). Thus, it is hardly possible that chorus emissions are responsible for a significant portion of the REP events seen by NOAA POES within the trapping zone. In fact, the similarity of the morphology as well as direct comparisons leads to suggestion that chorus emissions are responsible for relativistic electron microbursts (e.g., *Lorentzen et al., 2001*), which are not a subject of this paper. The equatorial magnetosonic emission occurrence and largest amplitudes have been also found in the dawn-noon sector (e.g., *Ma et al., 2013*) where REP on NOAA POES have the minimal occurrence.

The plasmaspheric hiss locates, statistically, on the day-afternoon side during quiet intervals and tends to expand to the night sector during disturbed intervals (*Meridith et al., 2004*). Also, the plasmaspheric hiss tends to intensify within the plasmaspheric plume and plume structures (*Summers et al., 2008; Chen et al., 2012*). The UHR waves are observed at all MLTs (*Kurth et al., 1979*). Thus, the plasmaspheric hiss and UHR waves could be responsible for significant part of REP events observed by NOAA POES.

The plasmaspheric plume is the region where both relativistic electrons and energetic protons might be scattered by EMIC waves (e.g., *Thorne and Kennel, 1971; Meredith et al., 2003*). Coincidence of energetic proton and relativistic electron precipitation is often considered as evidence of REP as result of the interaction with EMIC waves (e.g., *Carson et al., 2012 and references there*). However, all REP events of our third group (REP associated with precipitating protons) also coincide with the precipitation of energetic electrons. The presence of simultaneous precipitation of energetic (>30 keV) electrons means that some other waves (besides EMIC waves) exist in the same place. Perhaps, just these waves scatter relativistic electrons. Closely spaced precipitation of energetic protons and electrons can be generated within a small-scale plasmaspheric plume structure due to interaction with EMIC waves and ELF-VLF waves, respectively. This has been suggested by *Yahnin et al.* (2006) and demonstrated by *Yuan et al.* (2012, 2013). In the case of sufficiently small cold plasma inhomogeneity the precipitation related to different waves should nearly coincide. Thus, the coincidence of the energetic proton and relativistic electron precipitation cannot be considered as undoubted evidence of the interaction with EMIC waves.

References

Carson, B.R., C.J. Rodger, and M.A. Clilverd (2012), POES satellite observations of EMIC-wave driven relativistic electron precipitation during 1998–2010, J. Geophys. Res. Space Physics, 118, 232–243, doi:10.1029/2012JA017998.

Chen, L., R.M. Thorne, and R.B. Horne (2009), Simulation of EMIC wave excitation in a model magnetosphere including structured high-density plumes, J. Geophys. Res., 114, A07221, doi:10.1029/2009JA014204.

Chen, L., R.M. Thorne, W. Li, J. Bortnik, D. Turner, and V. Angelopoulos (2012), Modulation of plasmaspheric hiss intensity by thermal plasma density structure, Geophys. Res. Lett., 39, L14103, doi:10.1029/2012GL052308.

Evans, D.S., and M.S. Greer (2004), Polar Orbiting Environmental Satellite Space Environment Monitor−2 Instrument Descriptions and Archive Data Documentation, NOAA Tech. Mem. 1.4, Space Environ. Lab., Boulder, Colorado.

Horne, R.B., M.M. Lam, and J.C. Green (2009), Energetic electron precipitation from the outer radiation belt during geomagnetic storms, Geophys. Res. Lett., 36, L19104, doi:10.1029/2009GL040236.

Imhof, W.L., Voss, H.D., Reagan, J.B., Datlowe, D.W., Gaines, E.E., Mobilia, J., 1986. Relativistic electron and energetic ion precipitation spikes near the plasmapause. Journal of Geophysical Research 91, 3077–3088.

Imhof, W.L., Voss, H.D., Mobilia, J., Datlowe, D.W., Gaines, E.E., 1991. The precipitation of relativistic electrons near the trapping boundary. Journal of Geophysical Research 96, 5619.

Jordanova, V. K., J. Albert, and Y. Miyoshi (2008), Relativistic electron precipitation by EMIC waves from self-consistent global simulations, J. Geophys. Res., 113, A00A10, doi:10.1029/2008JA013239.

Kurth, W.S., J.D. Graven, L.A. Frank, and D.A. Gurnett (1979), Intense electrostatic waves near the upper hybrid resonance frequency, J. Geophys. Res., 84, 4145-4164.

Lorentzen, K.R., J. B. Blake, U.S. Inan, and J. Bortnik (2001), Observations of relativistic electron microbursts in association with VLF chorus, J. Geophys. Res., 106, 6017-6027.

Ma, Q., W. Li, R. M. Thorne, and V. Angelopoulos (2013), Global distribution of equatorial magnetosonic waves observed by THEMIS, Geophys. Res. Lett., 40, 1895–1901, doi:10.1002/grl.50434.

Meredith, N.P., R.M. Thorne, R. B. Horne, D. Summers, B. J. Fraser, and R. R. Anderson, Statistical analysis of relativistic electron energies for cyclotron resonance with EMIC waves observed on CRRES, J. Geophys. Res., 108(A6), 1250, doi:10.1029/2002JA009700, 2003.

Meredith, N.P., R.B. Horne, R.M. Thorne, D. Summers, and R. R. Anderson (2004), Substorm dependence of plasmaspheric hiss, J. Geophys. Res., 109, A06209, doi:10.1029/2004JA010387.

Meredith, N.P., R. B. Horne, J. Bortnik, R.M. Thorne, L. Chen, W. Li, and A. Sicard-Piet (2013), Global statistical evidence for chorus as the embryonic source of plasmaspheric hiss, Geophys. Res. Lett., 40, 2891–2896, doi:10.1002/grl.50593.

Millan R.M., Thorne R.M. (2007), Review of radiation belt relativistic electron losses. J. Atmos. Sol.-Terr. Phys. 69(3), 362–377.

Nakamura, R., M. Isowa, Y. Kamide, D. N. Baker, J. B. Blake, and M. Looper (2000), SAMPEX observations of precipitation bursts in the outer radiation belt, J. Geophys. Res., 105(A7), 15875–15885, doi:10.1029/2000JA900018

Rodger, C.J., M. A. Clilverd, J.C. Green, and M.M. Lam (2010), Use of POES SEM□2 observations to examine radiation belt dynamics and energetic electron precipitation into the atmosphere, J. Geophys. Res., 115, A04202, doi:10.1029/2008JA014023.

Sergeev, V.A., Tsyganenko, N.A. (1982), Energetic particle losses and trapping boundaries as deduced from calculations with a realistic magnetic field model. Planetary and Space Science 30, 999.

Shklyar, D.R., and B. Kliem (2006), Relativistic electron scattering by electrostatic upper hybrid waves in the radiation belt, J. Geophys. Res., 111, A06204, doi:10.1029/2005JA011345.

Summers, D., B. Ni, N. P. Meredith, R.B. Horne, R.M. Thorne, M.B. Moldwin, and R.R. Anderson (2008), Electron scattering by whistler-mode ELF hiss in plasmaspheric plumes, J. Geophys. Res., 113, A04219, doi:10.1029/2007JA012678.

Thorne, R.M. (2010), Radiation belt dynamics: The importance of wave-particle interactions, Geophys. Res. Lett., 37, L22107, doi:10.1029/2010GL044990.

Thorne, R.M., Kennel, C.F., 1971. Relativistic electron precipitation during magnetic storm main phase. J. Geophys. Res., 76, 4446.

Wang, Z., Z. Yuan, M. Li, H. Li, D. Wang, H. Li, S. Huang, and Z. Qiao (2014), Statistical characteristics of EMIC wave-driven relativistic electron precipitation with observations of POES satellites: Revisit, J. Geophys. Res. Space Physics, 119, 5509–5519, doi:10.1002/2014JA020082.

Yando, K., R. M. Millan, J. C. Green, and D. S. Evans (2011), A Monte Carlo simulation of the NOAA POES Medium Energy Proton and Electron Detector instrument, J. Geophys. Res., 116, A10231, doi:10.1029/2011JA016671.

Yahnin A.G. and Yahnina T.A. Energetic Proton Precipitation Related to Ion-Cyclotron Waves, J. Atmos. Solar-Terr. Phys., Vol 69/14, pp 1690-1706, 2007 (doi: 10.1016/j.jastp.2007.02.010).

Yahnin, A.G., T.A. Yahnina, A.G. Demekhov (2006), Interrelation between localized energetic particle precipitation and cold plasma inhomogeneities in the magnetosphere, Geomagnetism and Aeronomy, 46 (3), 332–338.

Yuan, Z., Y. Xiong, Y. Pang, M. Zhou, X. Deng, J. G. Trotignon, E. Lucek, and J. Wang (2012), Wave-particle interaction in a plasmaspheric plume observed by a Cluster satellite, J. Geophys. Res., 117, A03205,doi:10.1029/2011JA017152.

Yuan, Z., Y. Xiong, D. Wang, M. Li, X. Deng, A. G. Yahnin, T. Raita, and J. Wang (2012), Characteristics of precipitating energetic ions/electrons associated with the wave-particle interaction in the plasmaspheric plume, J. Geophys. Res., 117, A08324, doi:10.1029/2012JA017783.